

In vitro bioactivity of Polyurethane/85S Bioglass composite scaffolds

Research Article

Lachezar Radev^{1*}, Darina Zheleva², Irena Michailova³

¹Department of Fundamental Chemical Technology,
University of Chemical Technology and Metallurgy,
Sofia 1756, Bulgaria

²Textile and Leather Department,
University of Chemical Technology and Metallurgy,
Sofia 1756, Bulgaria

³Department of Silicate Technology,
University of Chemical Technology and Metallurgy,
Sofia 1756, Bulgaria

Received 20 October 2012; Accepted 15 April 2013

Abstract: In the present work Polyurethane (PU)/ Bioglass (BG) composite materials were synthesized with different content of BG (10 and 20 mol.%) as filler. The 85S Bioglass was synthesized *via* polystep sol-gel method. The chemical composition of BG is 85SiO₂-10CaO-5P₂O₅ (wt.%). The synthesis of PU was carried out by a two-step polyaddition reaction. The 85S BG was added *in situ* during the polymerization reaction. *In vitro* bioactivity of the prepared composites was examined in the presence of 1.5 SBF for 7 days in static conditions. The structure of synthesized PU/BG composites before and after *in vitro* test was determined by XRD, FTIR and SEM. XRD of the samples before *in vitro* test proved that the phase of γ -Ca₂P₂O₇ in the PU/20BG is visible. FTIR revealed the presence of urethane bond between OH⁻ (from BG) and NCO groups (from PU). Based on FTIR results after *in vitro* test in 1.5 SBF solutions, A/B-carbonate containing hydroxyapatite (CO₃HA) was formed. XRD proved that HA was formed on the surface of the samples, but Ca₂P₂O₇ does not undergo any changes in the 1.5 SBF solution. SEM depicted the nano-HA agglomerated in spherical particles after immersion in 1.5 SBF for 7 days.

Keywords: Scaffolds • Polyurethane • Bioglass • In vitro bioactivity
© Versita Sp. z o.o.

1. Introduction

Bioactive glass (BG) in the composition with biodegradable polymers have emergent recently as new class of bioactive materials with applications from implants to tissue engineering [1]. They have been on the one hand as regards, hard tissue engineering, BG have been proposed as bone graft materials which have a large range of applications [2,3]. On the other hand, the sol-gel glass in 85SiO₂-10CaO-5P₂O₅ system has been traditionally used for hard tissue repair, due to their highly bioactive behavior [4-7]. Above the traditional of silica based BG, phosphate based scaffold, able to resorb the same time as the bone is repaired, have been recently proposed.

In the previous years, polymer/ceramic (glass) porous composites have attracted increasing interest as scaffolds for bone tissue engineering, as described in [8]. Polyurethane (PU) is a biocompatible and biodegradable polymer with very good physical and mechanical properties [9].

Two classes of composite scaffolds have been fabricated and investigated in the presence of BG and PU: the first one – polymer based scaffolds, coated with glass (ceramic) particles [10,11] and the second one – polymer, coated glass (ceramic) scaffolds [12]. Concerning the composite scaffolds fabricated by using a PU only two types of glasses have been tested: Bioglass® [13] and Cell 2 silica based glass-ceramics with nominal composition 45%SiO₂-3%P₂O₅-26%CaO-

* E-mail: l_radev@abv.bg

7%MgO-15%Na₂O-4%K₂O (mol.%) [8]. In series of papers *in vitro* bioactivity of nano-hydroxyapatite (n-HA)/PU composites have been investigated [14-17]. There, the very challenging question is: did the authors observe a covalent bond between isocyanate and HA? Long time ago, Liu *et al.* [18] and Dong and his co-workers [19] investigated the reactivity between isocyanate with HA and with calcium hydrogenphosphate (CHP). Based on the obtained results, they concluded that there was (i) a covalent bond between isocyanate and HA, and (ii) a urethane linkage between hexamethylen diisocyanate and CHP. The others also showed, that the OH⁻ groups at the surface of HA have reactivity towards organic functional groups [14,16,17,20].

In this work, PU/BG composites are developed as a promising way for bone tissue engineering. The scaffolds were produced by mixing method. *In vitro* bioactivity of the prepared PU/BG composites were evaluated in the 1.5 SBF solution at 37°C for 7 days. FTIR and SEM were used as characterization techniques of the new scaffolds.

2. Experimental procedure

2.1. Materials

BG in the SiO₂-CaO-P₂O₅ system was used as filler. This glass was produced *via* sol-gel method. The composition of the prepared glass is: 85SiO₂-10CaO-5P₂O₅ (mol.%). CaO (Merck), Tetraethylorthosilicate, TEOS (Aldrich) and H₃PO₄ (Merck) was used as sources. CaO was heated at 500°C for 12 h before use.

To prepare the composites, appropriate quantities of BG powder were added to the polymer solution to yield composites with different concentration of BG (10 and 20 wt.%).

2.2. Polyurethane synthesis

The polyurethanes are polymers which are prepared by two-step polyaddition reaction. Reagents involved in the synthesis of polyurethane foams are following: 4,4'-diisocyanate (MDI), from Aldrich, with melting point 40°C, density 1,230 g cm⁻³; Lupranol 2095, from BASF, high reactive trifunctional polyether with hydroxyl groups, molecular mass 4800, hydroxyl number of 35 and viscosity 850 mPa.s; 1,4- butanediol (BD) as chains extender; water as expanding agent.

The process of preparing of polyurethane foam take place in two stages: (i) to the polyol component (Lupranol 2095) at amount of 10 g, add a few drops of water and stirred vigorously. After that this polyol mixture is added to the calculated stoichiometric amount of isocyanate

(MDI) – 1 g followed by vigorous stirring again. The synthesis reaction proceeds at 50°C during 30 min. The next stage (ii) is addition of chain extender (1,4-butanediol) for the augmentation the molecular mass. The foaming reaction starts seconds after mixing of the components.

2.3. Bioglass synthesis

The 85S powder as the inorganic part of the composites has been synthesized using a polystep sol-gel method. The chemical composition of the prepared sol is described as 85SiO₂-10CaO-5P₂O₅ (mol.%).

The first step was to prepare SiO₂ sol from TEOS. TEOS was stirred under a mixed solvent of C₂H₅OH and H₂O with a very small amount of HCl as a catalyst in a volume ratio of TEOS: C₂H₅OH: H₂O: HCl=1:1:1:0.01. After identifying a transparent solution of the above mixture after 1 hour, a mixture of calcium phosphate (CP) was added under intensive stirring.

The second step was to prepare the CP solution by mixing of Ca(OH)₂ and H₃PO₄ at alkaline pH. This CP solution was added to the SiO₂ sol stirring constantly for 24 hours. The produced mixed sol was gelated at 120°C for 12 hours and then stabilized at 700°C for 3 hours.

2.4. Synthesis of the composites

The synthesis of composites based on PU/BG occurs in the same way as pure polyurethane, only to the polyol component (Lupranol 2095) add 1.5 g BG, which is 10% (or 3.0 g bioglass, which is 20%) compared to polyurethane content and add a few drops of water and therefore stirring intensively. The composite between PU and 10 wt.% BG was named PU/10BG and the composite with 20 wt.% BG was named PU/20BG, respectively.

After that the mixture are added to the calculated stoichiometric amount of isocyanate (MDI) – 1 g and follows intensive stirring again. The synthesis reaction proceeds at 50°C during 30 min. The next stage is addition of chain extender (1,4-butanediol) for the augmentation the molecular mass. The foaming reaction starts seconds after mixing the components.

2.5. Bioactivity essay

Bioactivity of the composites obtained was evaluated by examining the apatite formation on their surfaces in 1.5 SBF solutions. The 1.5 SBF was prepared from different reagents as follow: NaCl=11.9925 g, NaHCO₃=0.5295 g, KCl=0.3360 g, K₂HPO₄•3H₂O=0.3420 g, MgCl₂•6H₂O=0.4575 g, CaCl₂•2H₂O=0.5520 g, Na₂SO₄=0.1065 g, and buffering at pH 7.4 at 36.5°C with 9.0075 g of *tris* (hydroxymethyl)

aminomethane (TRIS) and 1M HCl in distilled water. A few drops of 0.5% NaN_3 was added to the 1.5SBF solution to inhibit the growth of bacteria [21]. After soaking the specimens were removed from the fluid, gently rinsed with distilled water, and then dried at 36.6°C for 12 h.

2.6. Methods for analysis

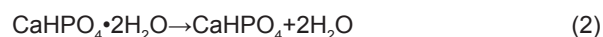
The structure and *in vitro* bioactivity of synthesized composites were monitored by X-ray diffraction (XRD), Fourier-transform infrared (FTIR) spectroscopy and scanning electron microscopy (SEM). XRD of the obtained composites were studied using Bruker D8 Advance with $\text{CuK}\alpha$ radiation at 15-60 (2 θ). FTIR transmission spectra for the obtained composites were recorded by using a Bruker Tensor 27 spectrometer with scanner velocity 10 kHz. KBr pellets were prepared by mixing ~1 mg of the samples with 300 mg KBr. Transmission spectra were recorded using MCT detector, with 64 scans and 1 cm^{-1} resolution. SEM (Jeol, JSM-35 CF, Japan) was used to ascertain the morphology and chemical constituents of the prepared composites before and after immersion in 1.5 SBF for 7 days at accelerating voltage of 15 kV.

3. Results and discussion

3.1. Characterization of the composites before *in vitro* test in 1.5 SBF

XRD data for the prepared PU/BG composites with different weight ratio of BG are presented in Fig. 1.

From the depicted Fig. 1 it can be seen that the presence of amorphous halo for PU (curve a) are quite visible. When the quantity of BG increased up to 20%, XRD observed the presence of well-defined crystalline phase of $\gamma\text{-Ca}_2\text{P}_2\text{O}_7$ (PDF 17-0499). The presence of this phase could be related to the formation of $\gamma\text{-Ca}_2\text{P}_2\text{O}_7$ during the stabilization of sol-gel glass at 700°C for 3 hours. From the obtained results we can conclude that the $\text{Ca}_2\text{P}_2\text{O}_7$ can produce according to the following reactions:



A typical FTIR spectrum of pure PU is shown in Fig. 2.

Fig. 2 spectrum revealed the presence of characteristics PU bands, N-H stretching vibration at

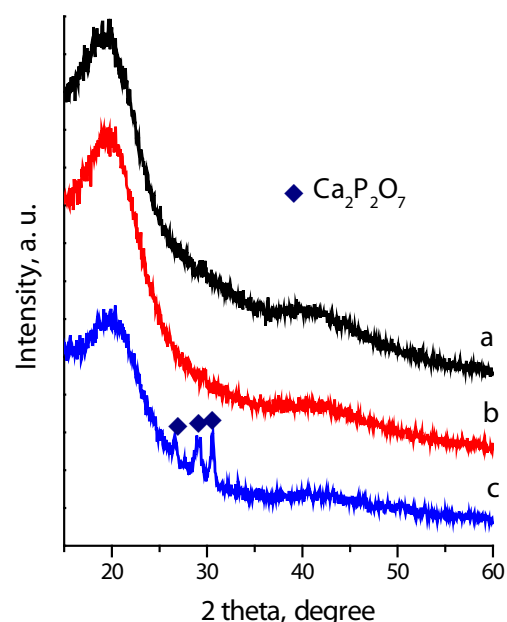


Figure 1. XRD for pure PU (a), PU/10BG (b) and PU/20BG (c).

3392 cm^{-1} , asymmetric and symmetric CH_2 stretching at 2924 and 2858 cm^{-1} , respectively [20]. The other modes of CH_2 vibrations are posited at 1410, 1373 and 1303 cm^{-1} [20,22]. The amide I band is presented at 1706 cm^{-1} [20,23]. The very strong δ (N-H) + ν (C-H) is located at 1510 cm^{-1} [20] and the strong δ (N-H) + ν (C-N) is posited at 1237 cm^{-1} [20,24]. The band at 1450 cm^{-1} is characteristic for the soft segments of PU. The absorbance at 1183 and 1100 cm^{-1} was attributed to ether bonds [20,25] and C-O-C stretching vibration band is seen at 1012 cm^{-1} [20,26]. On the other hand, Fig. 2 FTIR spectrum shows the presence of 1776-1597 cm^{-1} which could be assigned to the urethane and/or polycaprolactone ester C-O group [20]. Moreover, the stretching bands at 1665 cm^{-1} and 1706 cm^{-1} are due to the absorption of hydrogen bonded C-O of urethane linkages [20,27,28]. In addition, the isocyanate group absorbs strongly at 2275 cm^{-1} [29].

FTIR spectrum of 85S bioactive glass is presented at Fig. 3.

As it is written in [30], the IR spectra of SiO_2 based glasses, reveal the presence of three main vibrational modes of the Si-O-Si groups in the region between 400-1300 cm^{-1} . In accordance with some infra-red data, the bands located in the range 1000-1300 cm^{-1} are associated with the Si-O-Si asymmetric stretching mode [31]. As could be seen from Fig. 2 FTIR spectrum of 85S sol-gel glass, this band is composed of two transverse modes: (i) a more intensive one, posited at 1098 cm^{-1} and a shoulder one, located at 1212 cm^{-1} . Furthermore, the band at 797 cm^{-1} could be identified as Si-O-Si

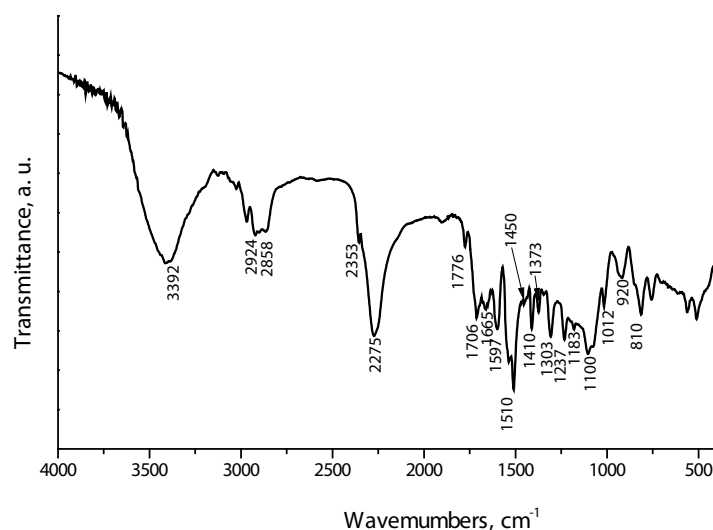


Figure 2. FTIR spectrum of pure PU.

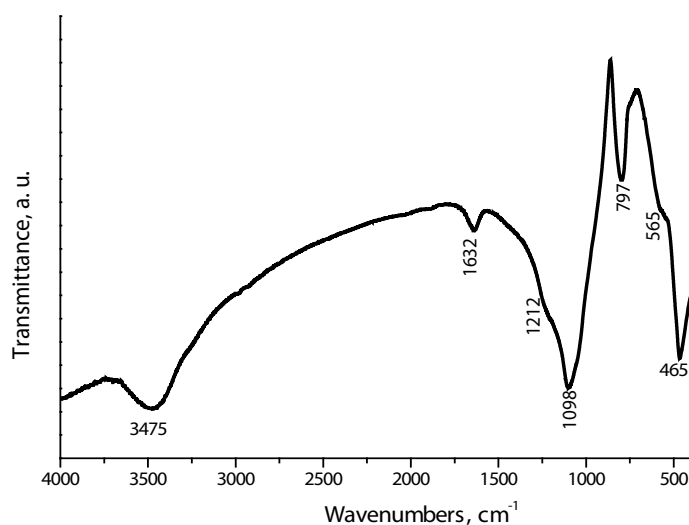


Figure 3. FTIR spectrum of pure 85S bioactive glass.

bending vibration. Finally, the band posited at 465 cm⁻¹ can be assigned to Si-O-Si rocking vibration [32-34]. The shoulder band at 565 cm⁻¹ could be ascribed to PO₄³⁻ bending mode in coincidence with Aguiar *et al.* [30].

The FTIR spectra of the synthesized composites between PU and BG, in which BG is in different weight ratio, are given in Fig. 4.

The PU in the composites was identified by the presence of some peaks: (i) urethane linkage at 3318 cm⁻¹ (●), for the sample with 20 wt.% BG (curve b), (ii) carbonyl vibration at 1705 (1703) cm⁻¹ and (iii) C-O-C vibration at 1098 (1103) cm⁻¹ (curves a and b). The peak with small intensity at 3318 cm⁻¹ (●) could be assigned to the NH-(C=O)-O-, which can be produced from

OH- (BG) and NCO-groups (PU). The presence of this peak (curve b) showed that a covalent bond between BG and PU was formed. This fact is in agreement with Khan *et al.* [20]. In addition, the peaks, centered at 3384 and 3470 cm⁻¹ are due to the stretching vibration of N-H for both composites [20,35].

From Fig. 4 FTIR spectra, we could also see that the intensity of the band, positioned at 2272 (2278) cm⁻¹ (●) for the two samples, slightly decreased (Fig. 4b). In a few words, when the quantity of BG increased, the intensity of NCO bond decreased. D. Tang *et al.* proved that the change in the intensity of this bond could be related with the formation of interpenetrating network between PU and unsaturated polyester (UP) [36]. In our case, we can conclude that the decreasing of the intensity of

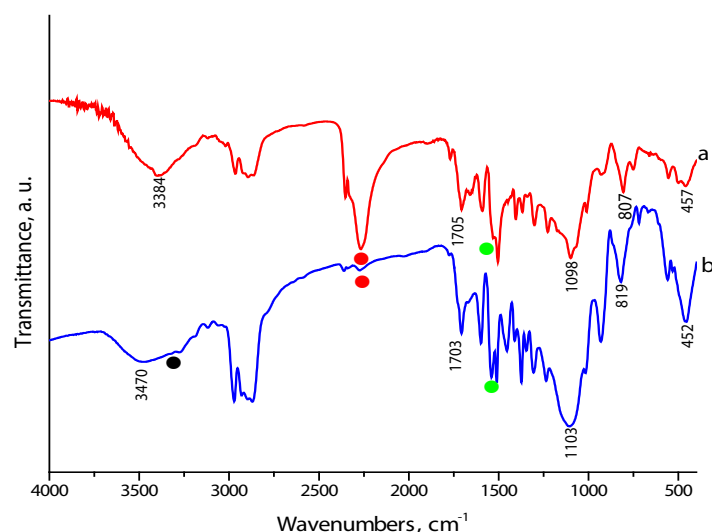


Figure 4. FTIR spectra for PU/10BG (a) and PU/20BG (b), before *in vitro* test.

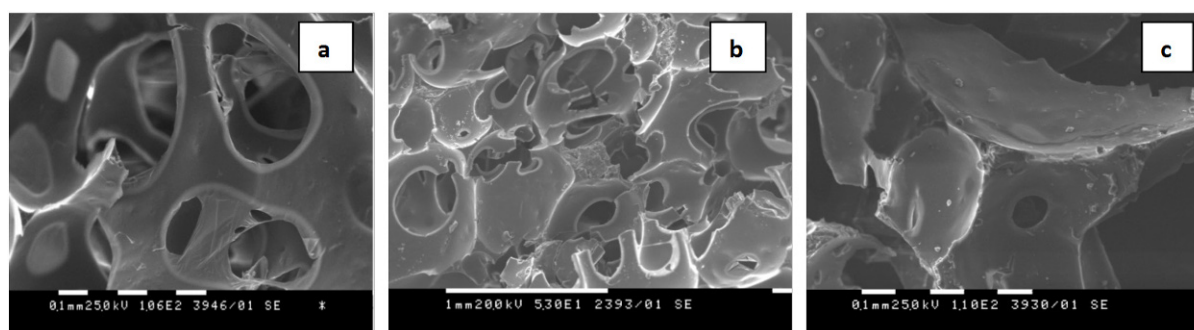


Figure 5. SEM of the PU (a), PU/10BG (b) and PU/20BG (c) before *in vitro* test.

NCO bond could be assigned to the formation of NH-(C=O)-O- bond between OH⁻ (from BG) and NCO-groups (from PU). As can be seen from the presented data, the isocyanate group has high activity. Moreover, in Fig. 4 FTIR spectra, we can be seen the presence of the peak, centered at 1536 (1539) cm⁻¹ (●). Khan *et al.* proved that the presence of this peak is indicative for urethane linkage [20]. It is evidence that the intensity of urethane bond increased with the increasing of the weight ratio of BG in the prepared composites. In addition, in the presented in Fig. 4 FTIR spectra we could not observe the presence of the bands, centered at ~1720 cm⁻¹, *i.e.*, the P-O-CO-NH bond was not observed [20].

It is already known, that the organic/inorganic composites for tissue engineering scaffolds are materials which exhibit foam like microporous structure.

Fig. 5 presents SEM micrographs for pure PU (Fig. 4a) and for PU/BG composites with 10 and 20 wt.% BG (Figs. 4b and 4c).

From the depicted SEM results, it can be seen that the pores are interconnected to allow continuous flow

of nutrients in the scaffold and can be populated with cells of various origin [14]. The PU/BG porous scaffolds (Figs. 4b and 4c) have not only macropores, but also a lot of micropores posited on the macroporous wall, which fulfill all of these criteria for an ideal scaffold [13,14]. As can be seen, the uniformly dispersed BG crystals are visible in the PU matrix.

3.2. Characterization of the composites after *in vitro* test in 1.5 SBF

The XRD diffraction patterns of the immersed samples with different quantity of BG are given in Figs. 6a and 6b.

The depicted X-ray diffraction data detects the presence of amorphous halo at 19.5 (2θ) and the γCa₂P₂O₇ (PDF 17-0499) and hydroxyapatite (PDF 09-0432). From the presented XRD results it is visible that (i) the crystallinity of Ca₂P₂O₇ phase of the immersed samples has no changes, *i.e.*, Ca₂P₂O₇ does not undergo dissolution in 1.5 SBF solution and (ii) the HA formation is a function of BG content into the composites.

FTIR of the synthesized composites after soaking in 1.5 SBF for 7 days is given in Fig. 7.

The FTIR spectra of the two composite materials after 7 days of soaking in 1.5 SBF showed that the intensities of the bands significantly decreased with increasing of the immersion time, compared with that of the control samples (Fig. 4). The decrease of the peaks intensities after *in vitro* test was attributed to the hydrolysis of the ester segments at the specimens' surface and SBF solution interface. This process should result in chain scission and dissolution of ester bonds in the solution [13]. On the other hand, the intensity of the bands of

the soaked samples (Fig. 5) increased with increasing the BG content in the synthesized composites. In the FTIR spectrum of PU/10BG after *in vitro* test some new peaks appear. The peaks at 1424 and 1461 cm^{-1} could be ascribed to the $\nu_3 \text{CO}_3^{2-}$ [37]. Others prove that the band, centered at 1461 cm^{-1} is indicative for A-type carbonate containing hydroxyapatite ($\text{A-CO}_3\text{HA}$) in which $\text{CO}_3^{2-} \rightarrow \text{OH}^-$ [38]. From the depicted in Fig. 7, curve a FTIR spectrum, the band posited at 1023 cm^{-1} became stronger and more visible. The increasing of the intensity of this band could be related with formation of crystalline phosphates after *in vitro* test [14,39]. In addition, this band is accompanied with a small $\nu_4 \text{PO}_4^{3-}$ peak, posited at 560 cm^{-1} . The presence of this doublet $\nu_4 \text{PO}_4^{3-}$ is characteristic for CO_3HA [40]. Furthermore, the well crystalline hydroxyapatite is also characterized by a band, positioned at $\sim 630 \text{ cm}^{-1}$ arising from OH^- liberation [40].

The FTIR spectrum of PU/20BG (Fig. 7, curve b) showed the presence of some peaks, centered at 1590, 1500 and 1446 cm^{-1} . In accordance with literature data, these peaks could be assigned to the presence of $\nu_4 \text{CO}_3^{2-}$ and $\nu_3 \text{CO}_3^{2-}$ in the different kinds of CO_3HA [38]. As mentioned above, the peak centered at 1446 cm^{-1} could be assigned to the presence of A/B-type CO_3HA [41]. Moreover, the peak at 608 cm^{-1} corresponds to $\nu_4 \text{PO}_4^{3-}$ symmetric phosphate vibration of the PO_4^{3-} ion. Furthermore, the shape of $\nu_3 \text{CO}_3^{2-}$ signal and the presence of C-O absorption band at 712 cm^{-1} also clearly indicate that detectable calcite is associated with CO_3HA [42].

Morphological properties of the PU/BG samples after soaking in 1.5 SBF for 7 days, observed by SEM at high magnifications, given in Fig. 8, indicate that soaking in

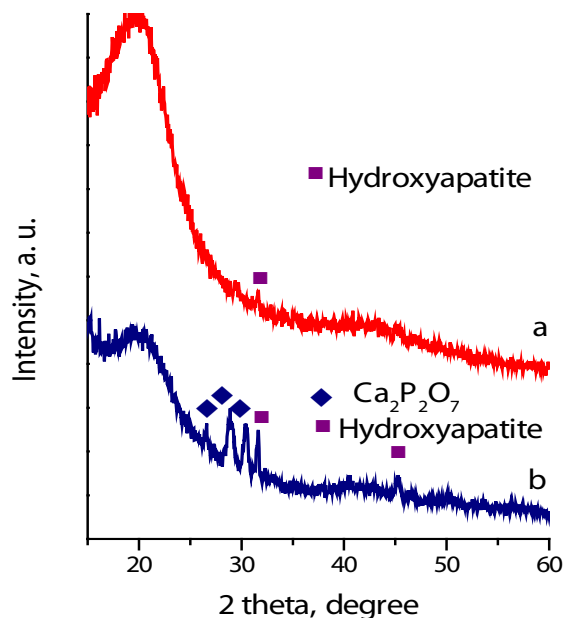


Figure 6. XRD for the PU/10BG (a) and PU/20BG (b) after *in vitro* test for 7 days.

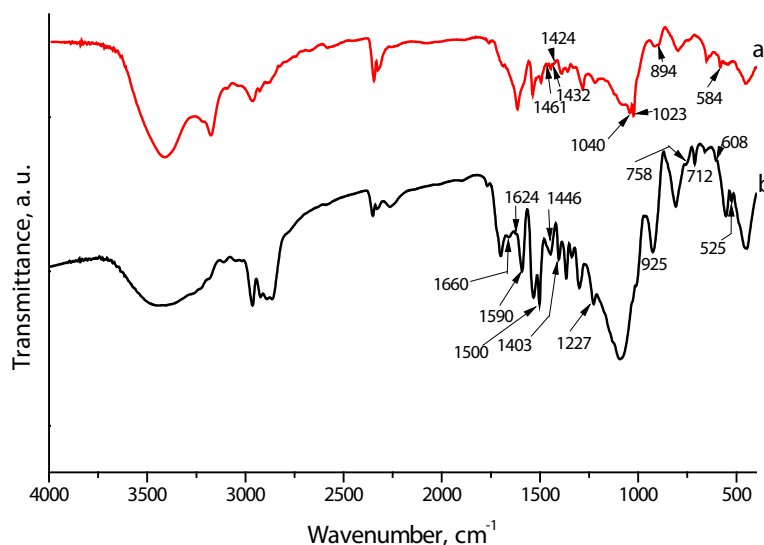


Figure 7. FTIR of the PU/10BG (a) and PU/20BG (b) after *in vitro* test in 1.5 SBF for 7 days.

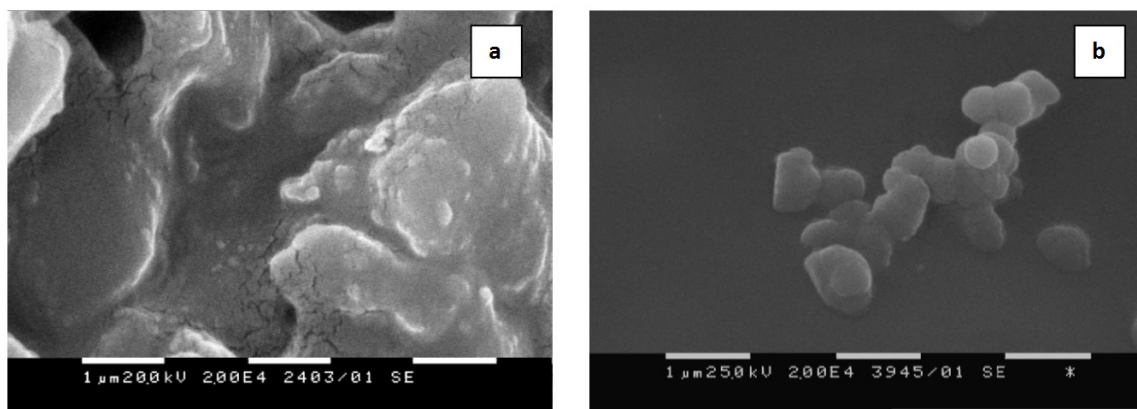


Figure 8. SEM of the PU/10BG (a) and PU/20BG (b) at $\times 20\,000$ after *in vitro* test for bioactivity for 7 days.

1.5 SBF solution for 7 days led to the formation of an apatite layer [14,15] on the surface of the samples.

SEM images, presented at Figs. 8a and 8b, show the differences of the surfaces of the samples. In the PU/10BG sample (Fig. 8a) the apatite covered the surface, but when the quantity of BG increased to 20 wt.% apatite particles with globular morphology can be formed. However, it needs more investigation to be proved.

4. Conclusions

The PU/BG composites in which BG is a nominal composition $85\text{SiO}_2\text{-}10\text{CaO-}5\text{P}_2\text{O}_5$ (wt.%) have been synthesized. The obtained PU/BG composites are prepared with 10 and 20 wt.% BG. XRD proved the presence of γ $\text{Ca}_2\text{P}_2\text{O}_7$ in the PU/20BG sample.

The presence of this phase could be ascribed to the decomposition reaction of CaHPO_4 at 700°C for 3 hours. FTIR revealed that the presence of (i) small peak, posited at $\sim 3318\text{ cm}^{-1}$ for PU/20BG sample and (ii) the increasing of the intensity of the band at 2272 (2278) cm^{-1} for the PU/10BG and for PU/20BG could be described to the presence of urethane linkage $\text{NH-}(\text{C=O})\text{-O-}$ between OH^- groups (from BG) and NCO groups (from PU). XRD of the immersed samples depict the presence of HA on the immersed samples. FTIR revealed the formation of A/B CO_3HA after *in vitro* test. SEM of the two samples depicted the presence of lamellar shaped nano-HA crystals agglomerated and formed spherical particles.

Based on the obtained results we can conclude that the prepared samples represent a novel family of scaffolds with potential application in bone tissue engineering.

References

- [1] A. Boccaccini et al., *Comp. Sci. Techn.* 70, 1764 (2010)
- [2] D.C. Fredericks et al., *Key Eng. Mater.* 218-220, 409 (2002)
- [3] C.E. Wilson et al., *Biomaterials* 27(3), 302 (2006)
- [4] D. Arcos et al., *Acta Biomaterialia* 7(7), 2952 (2011)
- [5] M. Alcaide et al., *Acta Biomaterialia* 6(3), 892 (2010)
- [6] H-S. Yun, J-W. Park, S-H. Kim, Y-J. Kim, J-H. Jang, *Acta Biomaterialia* 7, 2651 (2011)
- [7] A. Garca, M. Cicundez, I. Izquierdo-Barba, D. Arcos, *Chem. Mater.* 21(22) 5474 (2009)
- [8] F. Baino, E. Verné, Ch. Vitale-Brovarone, *J. Mater. Sci.: Mater. Med.* 20, 2189 (2009)
- [9] K. Bouchemal et al., *International Journal of Pharmaceutics* 269(1), 89 (2004)
- [10] M. Bil et al., *Biomed. Mater.* 2(2), 93 (2007)
- [11] M.- N. Huang, Y.- L. Wang, Y.- F. Luo, *J. Biomed. Sci. Eng.* 2, 36 (2009)
- [12] D.M. Yunos, O. Bretcanu, A.R. Boccaccini, *J. Mater. Sci.* 43, 4433 (2008)
- [13] J.L. Ryszkowska, M. Auguścik, A. Sheikh, A.R. Boccaccini, *Comp. Sci. Techn.* 70, 1894 (2010)
- [14] Zh. Dong, Y. Li, Q. Zou, *Appl. Surf. Sci.* 255(12), 6087 (2009)
- [15] G. Ciobanu, D. Ignat, C. Luca, *Chem. Bull. POLITECHNIKA Univ. Timisoara*, 54(68), 57 (2009)
- [16] A. Asefnejad, A. Behnamghader, M. Khorasani, B. Farsadzadeh, *Int. J. Nanomed.* 6, 93 (2011)
- [17] A.B. Martinez-Valencia et al., *Int. J. Phys. Sci.* 6(11), 2731 (2011)

- [18] Q. Liu, J.R. Wijn, D. Bakker, C.A. Blitterswijk, *J. Mater. Sci.: Mater. Med.* 7(9), 551 (1996)
- [19] G.Ch. Dong et al., *Biomaterials* 22(23), 3179 (2001)
- [20] A.S. Khan et al., *Acta Biomaterialia* 4(5), 1275 (2008)
- [21] G.Falini, S. Fermani, B. Palazzo, N. Roveri, *J. Biomed. Mater. Res.* A87(2), 470 (2008)
- [22] K. Gorna, S. Gogolewski, *Polym. Degrad. Stabil.* 75(1), 113 (2002)
- [23] E. Ayres, R.L. Oréfice, M.I. Yoshida, *Eur. Polym. J.* 43(8), 3510 (2007)
- [24] G. Wang, Ch. Zhang, X. Guo, Zh. Ren, *Spectrochimica Acta Part A: Molecular and Biomolecular Spectroscopy* 69 (2), 407 (2008)
- [25] J.Guan, M.S. Sacks, E.J. Beckman, W.R. Wagner, *J. Biomed. Mater. Res.*, A 61(3), 493 (2002)
- [26] (26) A.K. Mishra, D.K. Chattopadhyay, B. Sreedhar, K. Raju, *Prog. Org. Coat.* 55(3), 231 (2006)
- [27] L-F. Wang, *Polymer* 48, 894 (2007)
- [28] Ch. Chen et al., *Polymer* 46, 11849 (2005)
- [29] M.J. Forrest, *Chemical Characterization of Polyurethanes* (Papra Review Reports, UK, 2001)
- [30] H. Aguiar, J. Serra, P. González, B. León, *J. Non-Cryst. Solids* 355, 475 (2009)
- [31] F. Galeener, P.H. Gaskell, J.M. Parker, E.A. Davis, In: P.H. Gaskell, J.M. Parker, E.A. Davis (Eds.), *The Structure of Non-Crystalline Materials* (Taylor and Francis, London, 1982) 337
- [32] J. Serra et al. *J. Non-Cryst. Solids* 332, 20 (2003)
- [33] H.Y. Jung et al., *J. Non-Cryst Solids* 351, 372 (2005)
- [34] R.S. Pryce, L.L. Hench, *J. Mater. Chem.* 14, 2303 (2004)
- [35] E.S. Jang et al., *J. Chem. Soc. Pak.* 33(4), 549 (2011)
- [36] D. Tang, L. Quang, Zh. Jin, L. Zhao, *J. Mater. Sci. Technol.* 21(4), 58 (2005)
- [37] Q. Zhao et al. *J. Non-Cryst. Solids* 358 (2), 229 (2012)
- [38] N.S. Chickerur, M.S. Tung, W.E. Brown, *Calcif. Tissue Int.* 32(1), 55 (1980)
- [39] H. Lin, W.-S. Seo, K. Kuwabara, K. Koumoto, *J. Ceram. Soc. Jpn.* 104(4), 291 (1996)
- [40] H. Ou-Yang, E.P. Paschalis, A.L. Boskey, R. Mendelsohn, *Biopolymers* 57(3), 129 (2000)
- [41] D.G. Nelson, J.D. Featherstone, *Calcif. Tissue Int.* 34, S69 (1982)
- [42] P. Regnier et al., *American Mineralogist* 79, 809 (1994)